

Hydrogenation of nitrobenzenes catalyzed by platinum nanoparticle core-polyaryl ether trisacetic acid ammonium chloride dendrimer shell nanocomposite

Ping Yang^{a,*}, Wei Zhang^a, Yukou Du^a, Xiaomei Wang^b

^a College of Chemistry and Chemical Engineering, Soochow University, Suzhou 215123, China

^b College of Materials Science and Engineering, Soochow University, Suzhou 215123, China

Received 2 May 2006; received in revised form 24 June 2006; accepted 26 June 2006

Available online 7 August 2006

Abstract

Platinum nanoparticle core-polyaryl ether trisacetic acid ammonium chloride dendrimer shell nanocomposites (Pt@G_n-NACl) were prepared and used as catalysts for hydrogenation of nitrobenzenes to anilines with molecular hydrogen under mild conditions. The as-prepared nanoparticles have mean particle size from 2.0 to 5.5 nm, depending on the molar ratio of the metal and the dendrimer. The Pt nanoparticles demonstrate near-monodisperse when the molar ratio of Pt and G₃-NACl is below 30. The interaction among three carboxyl groups terminated at the dendron and the metallic core keeps the Pt nanoparticles from agglomerating. The colloidal solution of Pt nanoparticles stabilized by the dendrimer, in which the molar ratio of Pt/G₃-NACl was less than 60, is stable without precipitation for several weeks. The dendrons attach to the metal core radially, and a substantial fraction of the surface of the metal nanoparticle is unpassivated and available for catalytic reactions. Turnover frequencies for the hydrogenation of nitrobenzenes to anilines change from 353 to 49 h⁻¹ depending on the dendrimer generation and substrates. The dendrimer catalysts are stable during the catalytic hydrogenation process and can be recovered by centrifugation and reused. The results suggest the effectiveness of polyaryl ether trisacetic acid ammonium chloride dendrimer as a stabilizer for the preparation of Pt nanoparticle catalysts. © 2006 Elsevier B.V. All rights reserved.

Keywords: Fréchet-type dendrimer; Platinum nanoparticles; Catalytic hydrogenation; Nitrobenzenes

1. Introduction

Using metallodendrimer as a catalyst has attracted increasing interest in recent years, since it is possible to tune the catalytic properties through tailoring the structure, size, shape, and solubility of dendrimers and to locate catalytic sites at the core or on the periphery [1–4]. The synthesis of organometallic dendrimers, transition-metal, and bimetallic nanoparticles encapsulated inside dendrimers in a variety of architectures as well as their catalytic properties have been reported by Crooks and several other research groups [5–9]. These organometallic dendrimers and dendrimer-encapsulated metal nanoparticles proved to be efficient catalysts for Heck reaction, shape selective epoxidation, alkene oxidation, Kharasch addition reaction, cyclocarbonylation, olefin hydroformation, and asymmetric and

symmetric hydrogenations [10–28]. Niu et al. [10] demonstrated that size-selective hydrogenation of olefins could be achieved by simply changing dendrimers' generation. Esumi et al. [11] reported the reduction reaction of 4-nitrophenol catalyzed by PAMAM- and PPI-metal nanocomposites. It was found that the PPI dendrimers-palladium nanocomposites showed the highest catalytic activity for the reduction of 4-nitrophenol; however, the catalytic reactions were carried out in the presence of NaBH₄. Fox and co-workers [14] reported that palladium-nanoparticle-cored dendrimers (Pd-G-3) could efficiently catalyze Heck and Suzuki reactions. The coupling reactions catalyzed by Pd-G-3 could be performed under homogeneous or heterogeneous conditions with high activity. One drawback of this kind of catalyst was that Pd-G-3 could not be employed as a catalyst for hydrogenation reactions, since the carbon–sulphur bonds in Pd-G-3 were broken under the hydrogenation conditions. Since we are interested in using metal nanoparticle-cored dendrimers as hydrogenation catalysts, we synthesized polyaryl ether aminediacetic acid dendrimer (G_n-NA) as the stabilizer for preparation

* Corresponding author. Tel.: +86 512 65880361; fax: +86 512 65880089.
E-mail address: pyang@suda.edu.cn (P. Yang).

of platinum-nanoparticle-cored dendrimer ($\text{Pt}@G_n\text{-NAs}$) [28]. The as-prepared catalyst proved to be effective for the catalytic hydrogenation of phenyl aldehydes to phenyl alcohols; however, the activity of the catalyst dropped in the following cycle reactions. This could be attributed to the metal nanoparticles agglomeration, since some of dendrons that attached on the nanoparticle surface were lost in the recycling process. Based on our previous study, the present paper deals with the synthesis of platinum-nanoparticle stabilized by polyaryl ether trisacetic acid ammonium chloride dendrimer, which possesses three carboxyl groups to interact with the metal nanoparticle, and catalytic hydrogenation of nitrobenzene derivatives with molecular hydrogen under mild conditions.

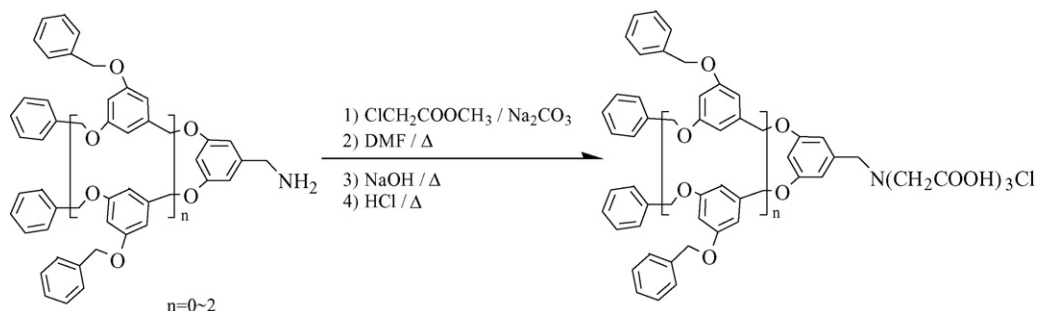
2. Experimental

2.1. Chemicals

3,3-Dihydroxybenzyl alcohol, 18-crown-6, benzyl bromide, and deuterated solvents were purchased from Acros Organic and used without further purification. Carbon tetrabromide and H_2PtCl_6 were obtained from Shanghai Chemical Reagents Company.

2.2. Synthesis of polyaryl ether trisacetic acid ammonium chloride dendron

Polyaryl ether benzylic bromide and polyaryl ether benzylic amine were synthesized using Fréchet method and an improved Gabriel method [29,30]. Polyaryl ether trisacetic acid ammonium chloride dendron with three carboxymethyl groups at the nitrogen atom ($G_n\text{-NACl}$) is readily accessible in a reaction of polyaryl ether amine with 6 molar equiv. of methyl chloroacetate. The synthesis of $G_n\text{-NACl}$ is demonstrated in Scheme 1. $G_n\text{-NH}_2$ (1.0 equiv.), methyl chloroacetate (6 equiv.), and anhydrous Na_2CO_3 (3.0 equiv.) mixed with 50 mL of DFM were heated at 90°C for 36 h under magnetic stirring. The resultant mixture was extracted with $\text{CH}_2\text{Cl}_2/\text{water}$ and then was mixed with an aqueous solution of NaOH and refluxed for 5 h. The mixture was cooled to room temperature and neutralized with hydrochloric acid. The light brown precipitate was purified by column chromatography. The yield for $G_1\text{-NACl}$ to $G_3\text{-NACl}$ is ca. 40–45%. The compounds were characterized by ^1H and ^{13}C NMR, respectively.



Scheme 1. Synthesis of $G_n\text{-NACl}$.

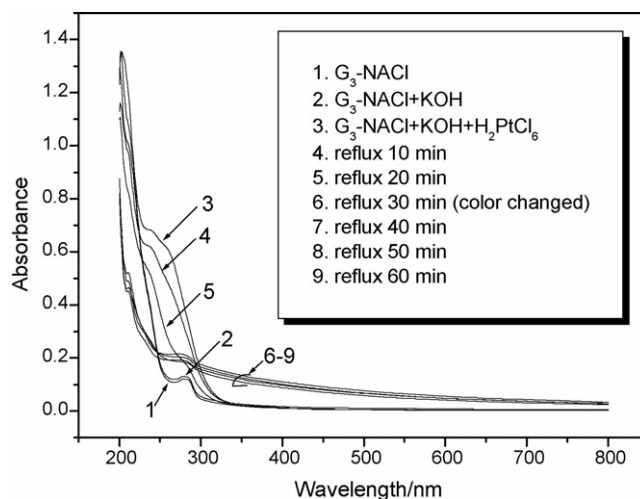


Fig. 1. UV-vis spectra of H_2PtCl_6 and $G_3\text{-NACl}$ dendrimer in an aqueous ethanol solution during the reduction process.

2.3. Preparation of platinum-nanoparticle-cored polyaryl ether trisacetic acid ammonium chloride dendrimer ($\text{Pt}@G_n\text{-NACls}$)

$\text{Pt}@G_n\text{-NACls}$ nanocomposites were prepared using an alcohol reduction method [31,32]. Briefly, 0.5 mmol of H_2PtCl_6 and a proper amount of $G_n\text{-NACl}$ (the range of the molar ratio of H_2PtCl_6 and $G_n\text{-NACl}$ is between 1 and 60) were at first mixed in aqueous ethanol (100 mL). The solution was adjusted to pH 9–10 under vigorous stirring at room temperature and then was heated to reflux for 2 h, resulting in a $\text{Pt}@G_n\text{-NACl}$ colloidal solution.

2.4. Hydrogenation reactions

Hydrogenation reactions were carried out in a 50 mL three-necked, round-bottomed Schlenk flask equipped with a hydrogen adapter, a dropping funnel, and a reflux condenser with a second adapter connected to a liquid paraffin bubbler. The system was purged with H_2 for 30 min before the reaction. Experiments were carried out by adding 10 mmol of substrate and a proper amount of catalyst dissolved in EtOH solvent through the dropping funnel under vigorous stirring conditions. All of the hydrogenation reactions were carried out at an atmospheric pressure. During the reaction process the reaction mixture was

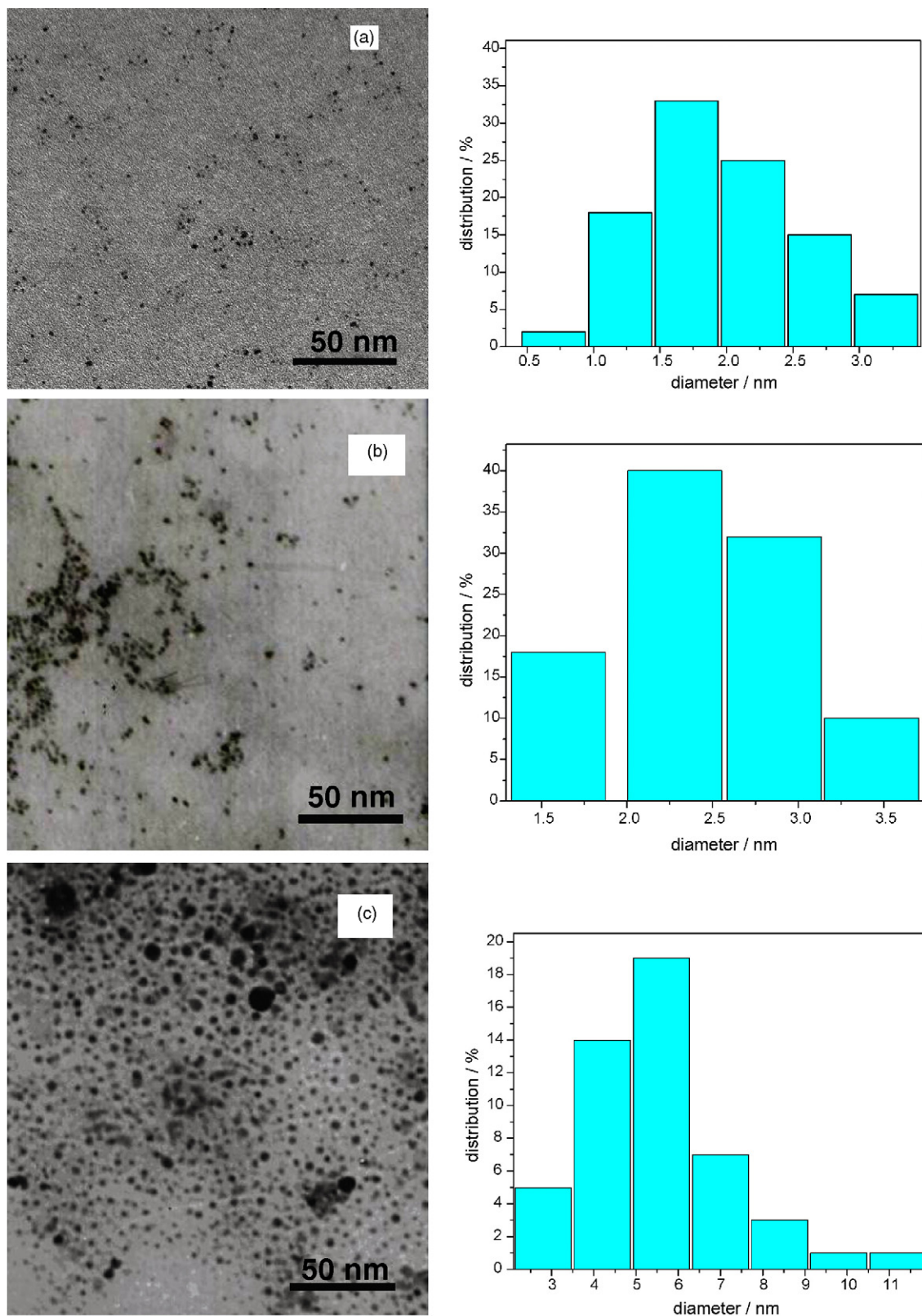


Fig. 2. Transmission electron micrographs of Pt@G₃-NaCl nanoparticles. The average size and standard deviation of the particles are 2.0 ± 0.6 , 2.4 ± 0.6 , and 5.5 ± 1.8 nm for the samples prepared in the molar ratio of Pt/G₃-NaCl at 1 (a), 30 (b), and 60 (c), respectively. The sample was prepared from an aqueous ethanol solution.

analyzed by GC-9800 gas chromatography equipped with an FID detector and an SE-30 packed column.

2.5. Characterization

Transmission electron microscopy (TEM) studies were conducted on a TECNAI-G20 electron microscope operating at an accelerating voltage of 200 kV. Samples for TEM analysis were prepared by dropping one drop of diluted Pt@G_n-NACl solution onto copper grids covered with Formvar and then dried in air, and placed into a desiccator prior to measurement. FTIR spectra were measured on a Nicolet Magna 550 spectrometer. UV–vis absorption spectra of samples were recorded on a TU1810 SPC spectrophotometer.

3. Results and discussion

Fig. 1 shows representative UV–vis spectra of the solution of G₃-NACl and H₂PtCl₆ in the reduction process. The UV–vis spectrum of the solution of G₃-NACl and H₂PtCl₆ demonstrates a broad band in the range of 240–320 nm before the reduction. At reflux temperature the intensity of the band gradually decreased in the first 30 min. The color of the solution remained light yellow and did not change obviously in this period. Then in a few minutes the color of the solution changed from light yellow to dark brown, indicating the formation of zero-valent platinum nanoparticles stabilized by G₃-NACl. The UV–vis spectrum of the solution revealed that the band in the range of 240–320 nm disappeared completely. After reduction the spectrum intensity of the colloidal solution increases as wavelength decreases in the range of 250–800 nm. The changes of the spectra may result from the interband transition of the encapsulated zero-valent metal particles [2]. Control experiments showed that the pH of the solution played an important role in the reduction process of PtCl₄²⁻ to Pt. When the pH of the solution was less than 9, the reduction process of PtCl₄²⁻ to Pt nanoparticle was not observed even refluxing the solution beyond 2 h; however, a Pt precipitate took place when the pH of the solution was beyond 10. Thus, chemical reduction of PtCl₄²⁻ in the presence of G_n-NACl to yield Pt@G_n-NACl nanoparticle was always carried out in the range of the pH between 9 and 10.

As-prepared platinum nanoparticle-cored dendrimers in different molar ratios of PtCl₄²⁻ and G₃-NACl have been characterized by transmission electron microscopy. Fig. 2 illustrates representative TEM images of Pt@G₃-NACl and the corresponding core-size histograms. As shown by TEM micrographs, the particles of Pt@G₃-NACl display near-monodisperse when the molar ratio of Pt and G₃-NACl is below 30. A clear increase in the size of Pt nanoparticles is observed as the molar ratio of Pt and G₃-NACl increases. When the molar ratio of H₂PtCl₆/G₃-NACl is 1, 30, and 60, the average diameters of Pt(0) particles are 2.0 ± 0.6, 2.4 ± 0.6, and 5.5 ± 1.8 nm, respectively. The core sizes of platinum particles exhibit a relatively wide size distribution when the molar ratio of Pt/G_n-NACl is 60. FTIR spectroscopy (Fig. 3) shows that there is ca. 20 cm⁻¹ peak shift to low wavenumber, comparing the C=O band stretching vibration of Pt@G₃-NACl with that of G₃-NACl in salt form. The significant peak shift

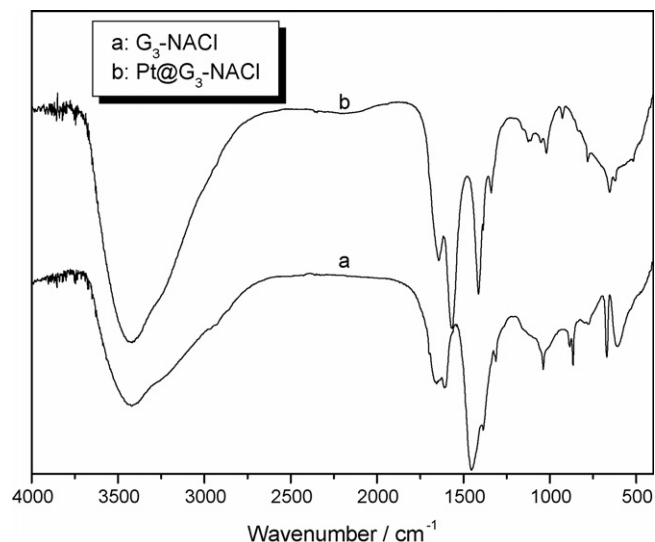
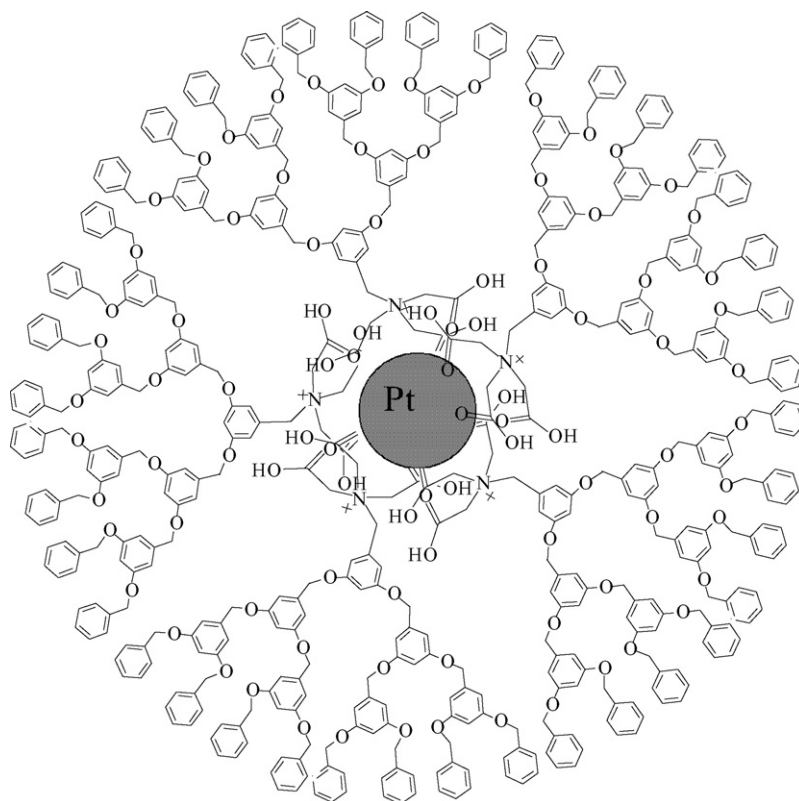


Fig. 3. FTIR spectra of G₃-NACl (a) and Pt@G₃-NACl (b).

for Pt@G₃-NACl is the evidence of the interaction between Pt cluster and carboxyl-terminated G_n-NACl [33]; this is because the C=O bond has less electron density, as the oxygen atom of the carbonyl interacted with the surface atom of the platinum nanoparticles. The supposed configuration of Pt@G₃-NACl is shown in Scheme 2. The interaction among three carboxyl groups terminated at the dendron and the metallic core keeps the Pt nanoparticles from agglomerating. The dendrons attach to the metal core radially; therefore, a substantial fraction of the surface of the metal nanoparticle is unpassivated and available for catalytic reactions [14].

Hydrogenation of nitrobenzenes to anilines was chosen to be the model reaction to investigate catalytic activities of the Pt@G_n-NACls with molecular hydrogen under one atmosphere pressure. In the reaction process the system remained homogeneous in the first 2 h, and then agglomeration of the catalyst was observed in the succedent reaction process; however, the agglomeration did not influence catalytic activity obviously. We guess that such an agglomeration is the result of the changing of the polarity of the solution. After the reaction the dendrimer catalyst can be isolated by centrifugation and redissolved in the mixed solvent. Thus, the agglomeration of the catalyst in reaction process is reversible.

As shown in Fig. 4, the Pt@G_n-NACls nanoparticles are found to be effective in the hydrogenation of nitrobenzenes. For the hydrogenation of *p*-nitrophenol, the Pt@G_n-NACl catalyst shows a gradual decrease of activities, with the dendrimer generation increasing from one to three. The same changing tendencies are also observed for the hydrogenation of other substrates. It seems that the substrates chosen for the hydrogenation can easily access the active sites through the low generation dendrimer shell with relative low steric hindrance and diffusion limitation. As the generation of the dendrimer increases, the conformation of Fréchet-type dendrimer changes from an extended to a more globular structure [34]. The relatively close shell of dendrimer in high generation could limit the accessibility of the

Scheme 2. The proposed configuration of Pt@G₃-NACl.

substrates into the active centers of platinum nanoparticle-cored dendrimer. This would lead to the decrease of the catalytic activity. Fig. 5 shows the temporal process of the hydrogenation of the nitrobenzene substrates catalyzed by Pt@G₃-NACl. The substitutional group of the substrate influences the catalytic activity in the same hydrogenation conditions. The Pt@G₃-NACl shows almost the same reactivity to *o*-nitroanisole and *p*-nitrophenol while showing relatively low activities to nitrotoluenes. The values of TOF are given in Table 1. The TOFs change from 353

to 49 h⁻¹ depending on the catalysts and the substrates used for the hydrogenation.

The hydrogenation of *o*-nitroanisole was employed to investigate the influence of molar ratio of substrate to catalyst on the catalytic activity. The results are demonstrated in Fig. 6. It can be concluded from Fig. 6 that the catalytic activity decreases with the increasing of the molar ratio of substrate to catalyst; however, the catalyst still shows nice catalytic activity; even the molar ratio of the substrate to the catalyst is as high as 1500.

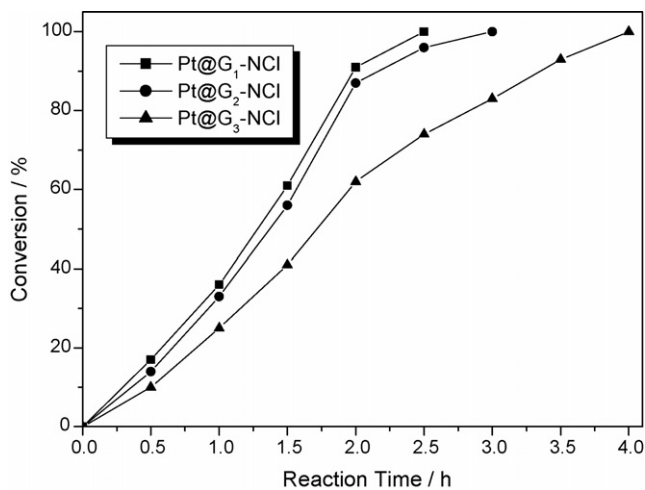


Fig. 4. Hydrogenation of *p*-nitrophenol catalyzed by Pt@G_{*n*}-NACl ($n_{\text{Pt}}/n_{\text{G}_n\text{-NACl}} = 30$). Reaction conditions— $n_{\text{substrate}}/n_{\text{catalyst}} = 900$; solvent: ethanol/water = 4 (v/v); reaction temperature: 40 °C.

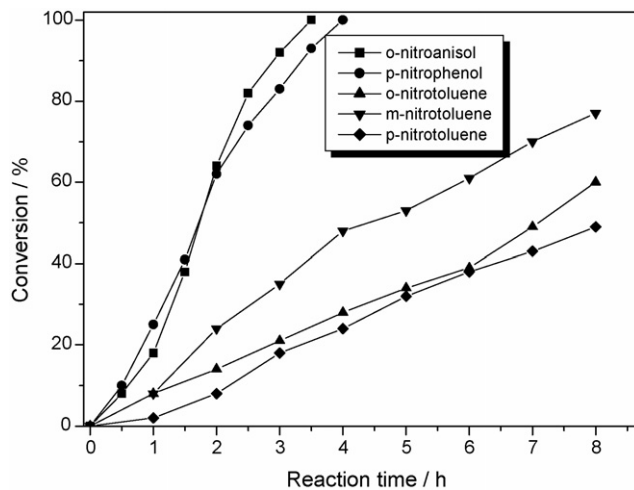
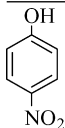
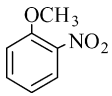
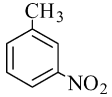
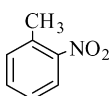
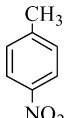


Fig. 5. Hydrogenation of nitrobenzenes to anilines catalyzed by Pt@G₃-NACl ($n_{\text{Pt}}/n_{\text{G}_3\text{-NACl}} = 30$). Reaction conditions— $n_{\text{substrate}}/n_{\text{catalyst}} = 900$; solvent: ethanol/water = 4 (v/v); reaction temperature: 40 °C.

Table 1
Catalytic activity of Pt@G_n-NACls for hydrogenation of nitrobenzenes to anilines

Substrate	Catalyst	Time (h)	Conversion (%)	TOF (mole product per mole Pt per hour)
	Pt@G ₁ -NACl	2.5	100	353
	Pt@G ₂ -NACl	3	100	326
	Pt@G ₃ -NACl	4	100	242
	Pt@G ₁ -NACl	3.5	100	295
	Pt@G ₂ -NACl	3.5	100	283
	Pt@G ₃ -NACl	3.5	100	232
	Pt@G ₁ -NACl	6	100	181
	Pt@G ₂ -NACl	7	100	158
	Pt@G ₃ -NACl	8	77	95
	Pt@G ₁ -NACl	6	100	153
	Pt@G ₂ -NACl	8	93	129
	Pt@G ₃ -NACl	8	60	64
	Pt@G ₁ -NACl	8	91	112
	Pt@G ₂ -NACl	8	69	90
	Pt@G ₃ -NACl	8	49	49

Reaction conditions—solvent: ethanol/water = 4 (v/v); catalyst: Pt@G_n-NACl ($n_{\text{Pt}}/n_{\text{G}_n\text{-NACl}} = 30$); $n_{\text{substrate}}/n_{\text{catalyst}} = 900$; reaction temperature: 40 °C.

After the hydrogenation the dendritic catalyst was separated from the reaction mixture by centrifugation and then, was redispersed into ethanol aqueous solution by ultrasonic treatment. The recovered catalyst exhibited higher activity in the first two recycles and retained good activity for all four cycles performed (Fig. 7).

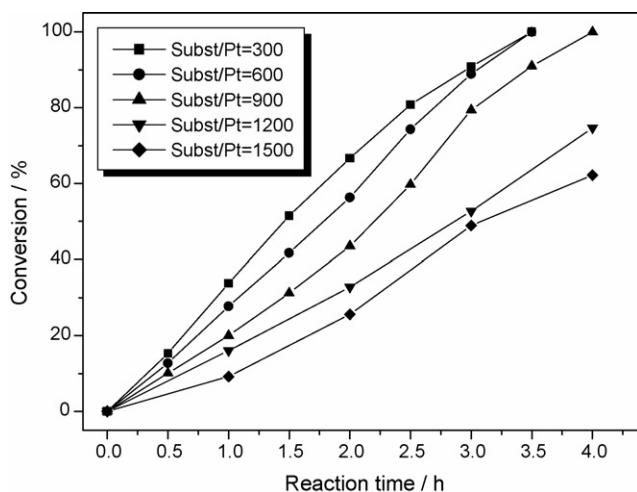


Fig. 6. The influence of the molar ratio of substrate/catalyst on the hydrogenation of *o*-nitroanisole reaction conditions. Catalyst: Pt@G₃-NACl ($n_{\text{Pt}}/n_{\text{G}_n\text{-NACl}} = 30$); solvent: ethanol/water = 4 (v/v); reaction temperature: 40 °C.

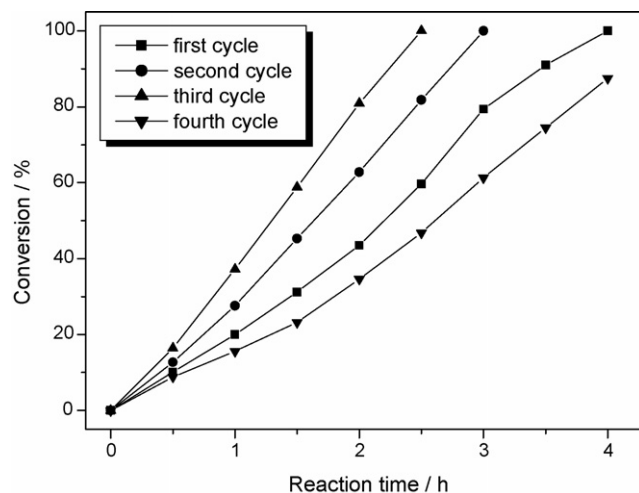


Fig. 7. Catalyst recycling for hydrogenation of *o*-nitroanisole. Reaction conditions—catalyst: Pt@G₃-NACl ($n_{\text{Pt}}/n_{\text{G}_n\text{-NACl}} = 30$); $n_{\text{substrate}}/n_{\text{catalyst}} = 900$; solvent: ethanol/water = 4 (v/v); reaction temperature: 40 °C.

Several research groups reported that higher activity was achieved for some bimetallic nanoparticles [12,15,35]. It is believed that an ensemble interaction between two different metals enhances the catalytic activity. The same cooperative interaction between platinum and gold bimetallic nanoparticle stabilized by G_n-NACl dendrons was also observed. Platinum and gold bimetallic nanoparticle demonstrated higher catalytic activity for the hydrogenation of nitrobenzenes. The influence of the cooperative interaction between two different metals to the activity is still under investigation.

4. Conclusions

Platinum nanoparticle core-polyaryl ether trisacetic acid ammonium chloride dendrimer shell nanocomposite proved to be an active and efficient catalyst for the hydrogenation of nitrobenzenes to anilines under an atmosphere pressure of H₂. The Pt nanoparticles capped by the dendrimer are stable during the catalytic hydrogenation process. The catalytic activity of the dendritic catalyst decreased with the increase of the generation of the dendrimer. The agglomeration of the catalyst in the last hydrogenation stage has the advantages of easy separation and reuse of the catalyst. The catalyst can be recovered and recycled at least four times.

Acknowledgements

The authors thank the National Natural Science Foundation of China (Grant Nos. 20543001, 50272024) and the Science Foundation of Jiangsu Province (BK2003031, 03KJB150115) for financial support.

References

- [1] D. Astruc, F. Chardac, Chem. Rev. 101 (2001) 2991.
- [2] R. Crooks, M. Zhao, L. Sun, V. Chechik, L. Yeung, Acc. Chem. Res. 34 (2001) 181.

- [3] R. Scott, O. Wilson, R. Crooks, *J. Phys. Chem. B* 109 (2005) 692.
- [4] G. Newkome, E. He, C. Moorefield, *Chem. Rev.* 99 (1999) 1689.
- [5] K. Gopidas, J. Whitesell, M. Fox, *J. Am. Chem. Soc.* 125 (2003) 6491.
- [6] O. Wilson, R. Scott, J. Garcia-Martinez, R. Crooks, *J. Am. Chem. Soc.* 127 (2005) 1015.
- [7] D. Volkmer, B. Bredenkötter, J. Tellenbröker, P. Kögerler, D. Kurth, P. Lehmann, H. Schnablegger, D. Schwahn, M. Piepenbrink, B. Krebs, *J. Am. Chem. Soc.* 124 (2002) 10489.
- [8] H. Lang, R. May, B. Iversen, B. Chandler, *J. Am. Chem. Soc.* 125 (2003) 14832.
- [9] L. Balogh, D. Tomalia, *J. Am. Chem. Soc.* 120 (1998) 7355.
- [10] Y. Niu, L. Yeung, R. Crooks, *J. Am. Chem. Soc.* 123 (2001) 6840.
- [11] K. Esumi, R. Isono, T. Yoshimura, *Langmuir* 20 (2004) 237.
- [12] Y. Chung, H. Rhee, *Catal. Lett.* 85 (2003) 159.
- [13] E. Rahim, F. Kamounah, J. Frederiksen, J. Christensen, *Nano Lett.* 1 (2001) 499.
- [14] K. Gopidas, J. Whitesell, M. Fox, *Nano Lett.* 3 (2003) 1757.
- [15] R. Scott, A. Datye, R. Crooks, *J. Am. Chem. Soc.* 125 (2003) 3708.
- [16] F. Gröhn, B. Bauer, Y. Akpalu, C. Jackson, E. Amis, *Macromolecules* 33 (2000) 6042.
- [17] M. Zhao, R. Crooks, *Angew. Chem. Int. Ed.* 38 (1999) 364.
- [18] M. Ooe, M. Murata, T. Mizugaki, K. Ebitani, K. Kaneda, *Nano Lett.* 2 (2002) 999.
- [19] M. Zhao, R. Crooks, *J. Am. Chem. Soc.* 120 (1998) 4877.
- [20] P. Bhyrappa, J. Young, J. Moore, K. Suslick, *J. Mol. Catal. A: Chem.* 113 (1996) 109.
- [21] Z. Yang, Q. Kang, H. Ma, C. Li, Z. Lei, *J. Mol. Catal. A: Chem.* 213 (2004) 169.
- [22] G. Koten, J. Jastrzebski, *J. Mol. Catal. A: Chem.* 146 (1999) 317.
- [23] R. Touzani, H. Alper, *J. Mol. Catal. A: Chem.* 227 (2005) 197.
- [24] Y. Huang, H. Zhang, G. Deng, W. Tang, X. Wang, Y. He, Q. Fan, *J. Mol. Catal. A: Chem.* 227 (2005) 91.
- [25] T. Mizugaki, M. Ooe, K. Ebitani, K. Kaneda, *J. Mol. Catal. A: Chem.* 145 (1999) 329.
- [26] G. Smith, S. Mapolie, *J. Mol. Catal. A: Chem.* 213 (2004) 187.
- [27] B. Yi, Q. Fan, G. Deng, Y. Li, L. Qiu, A. Chan, *Org. Lett.* 6 (2004) 1361.
- [28] Y. Du, W. Zhang, X. Wang, P. Yang, *Catal. Lett.* 107 (2006) 177.
- [29] C. Hawker, J. Fréchet, *J. Am. Chem. Soc.* 112 (1990) 7638.
- [30] J. Sheehan, W. Bolhofer, *J. Am. Chem. Soc.* 72 (1950) 2786.
- [31] J. Youk, J. Locklin, C. Xia, M. Park, R. Advincula, *Langmuir* 17 (2001) 4681.
- [32] H. Hirai, Y. Nakao, N. Toshima, *J. Macromol. Sci. Chem. A* 13 (1979) 727.
- [33] J. Petroski, M. El-Sayed, *J. Phys. Chem. A* 107 (2003) 8371.
- [34] C. Hawker, K. Wooley, J. Fréchet, *J. Am. Chem. Soc.* 115 (1993) 4375.
- [35] P. Lu, T. Teranishi, K. Asakura, M. Miyake, N. Toshima, *J. Phys. Chem. B* 103 (1999) 9673.